COMPUTER VISION AND IMAGE UNDERSTANDING
Vol. 63, No. 2, March, pp. 367–379, 1996
ARTICLE NO. 0026

The Curve Axis

DORON SHAKED*

Hewlett–Packard, Israel Science Center, Technion City, Haifa 32000, Israel

AND

ALFRED M. BRUCKSTEIN

Department of Computer Science, Center for Intelligent Systems, Technion, Haifa 32000, Israel

Received October 7, 1994; accepted January 10, 1995

In this paper we examine various aspects of the medial axis representation of shapes, resulting in a novel, highly accurate skeletonization algorithm suitable for shapes with parametrically described boundaries such as, for example, polygons or ''spline''-gons. The medial axis representation is first shown to be efficient in calculating local boundary features. Then the problem of deciding whether an axis-like function is indeed an axis of a shape is addressed, and two necessary and locally sufficient restrictions on axis functions are derived. The proposed skeletonization approach is based on another result which shows that the medial axis is the solution of a system of first order differential equations. The new skeletonization algorithm provides a discrete parametric representation of the axis for smooth shapes, the input to the algorithm being a parametric description of the shape boundary. Skeletonization examples using the proposed algorithm are presented. © 1996 Academic Press, Inc.

1. INTRODUCTION

The medial axis of a planar shape consists of the locus of centers of maximal discs in the shape, and of their corresponding radii. A maximal disc in the shape is a disc contained in the shape such that no other disc in the shape contains it [2]. The medial axis is considered an attractive representation of the shape. It is a lossless representation, and its planar part (or so-called Skeleton) often provides an intuitively appealing thin version of the shape.

Skeletonization is defined as a process that finds the medial axis of a given shape. It is also sometimes referred to as ''The Medial Axis Transform'' of a shape. The medial axis is a highly unstable shape feature; i.e., similar shapes may have very different axes. Since the digitization process often reduces similar shapes to the same set of pixels, it should be no surprise that skeletonization algorithms suffer from many implementation problems. Those problems follow mainly from various implicit assumptions about the pre-image of the digital shape. Some skeletonization algorithms stress this point by incorporating parameters setting the scale at which the shape should be interpreted, e.g., [1, 7].

Most skeletonization algorithms are area oriented. Those algorithms refer to and use pixels inside the shape. Their complexity is therefore proportional to the shape area. On the other hand, boundary oriented skeletonization algorithms refer to and use only boundary descriptors. Their complexity is potentially lower. Boundary oriented skeletonization algorithms traditionally assume that the pre-image (i.e., the image before digitization) was a polygon. Skeletonization relying on boundary descriptions has been addressed by Montanari [13] and by Lee [11], who suggested exact solutions for polygonal shapes. Some good algorithms approximating the exact solutions were suggested by Bookstein [4] and by Brandt *et al.* [5].

Due to the inherent edginess of polygonal shapes, the medial axes of polygonal approximations of a shape are quite different from each other and from the axes of its smoother approximations. In contrast to edgy (e.g., polygonal) models of shapes, smooth models have axes that are much more stable. Skeletonization from smooth boundary descriptors is discussed in the CAD literature. Analytical solutions to the case where the boundary is an ''arc-gon,'' i.e., a sequence of circular arc segments, was suggested by Persson [14]. In [17] Yap and Alt assert that an analytical solution for more general boundaries exists; however, it is impractical. They show that the axis curve of boundary segments with algebraic degree m is of algebraic degree $16m^2$. Recently Kimmel *et al.* have proposed a pixel driven, boundary oriented skeletonization based on a numerical

* Work done while in the Department of Electrical Engineering at the Technion.

1077-3142/96 $18.00

solution for the distance map of curve segments [10]. In the sequel we present a novel skeletonization algorithms for shapes with parametric smooth boundaries.

The new skeletonization algorithm is derived from a connection between the parametric descriptions of the boundary and the axis described via parametric curves. In the paper we analyze this connection and address three questions:

• Can we transform the axis representation of a shape into its boundary representation? Due to the ease of the transformation from the axis to an explicit representation of the spatial contents of the shape, this question has not gained a lot of interest since the initial work of Blum and Nagel [3]. Blum and Nagel were mainly interested in extracting boundary features from the axis, rather then a full boundary representation. While the feature extraction in [3] is based on geometric considerations, the algebraic boundary representation proposed herein makes possible the extraction of the basic features as well as more complex features having less obvious geometric meanings. Similar algebraic representations are used by Bruce and Giblin [6] to derive the generic forms of continuously deforming symmetry sets, and by Ponce [15] to compare different types of ribbons.

• Is there an easy way to tell whether a given axis representation is legal? By a legal axis function we mean a function that is indeed the axis of some shape, and by an ''easy way'' we mean avoiding an attempt to reconstruct the corresponding shape. This problem has been addressed previously by Rosenfeld [16]. Rosenfeld argued that ultimately some reconstruction process has to be carried out, in order to approve a proposed axis function. He also indicated that in some cases it is possible to detect an illegal axis function by some local inspection of the axis. We present two local conditions for an axis function to be legal, and prove that they are sufficient local conditions. All further investigations would have to be of a global nature, involving some kind of shape or boundary reconstruction.

• Can we transform a boundary representation of a shape to its axis representation? Or in other words, does this new look at axis representation also point to a new way to skeletonize shapes with smooth boundaries? We show that the medial axis is the solution to a system of first order ordinary differential equations driven by the boundaries. These equations indeed form the basis for a highly accurate skeletonization algorithm.

Equations and insights from the answers to the three questions above are incorporated in the novel skeletonization algorithm introduced toward the end of this paper. The system of equations describing the skeletonization is highly unstable; therefore we supplement them with equations suggested by Giblin and Brassett [8], which provide the necessary stabilization of the skeletonization process. The restrictions on legal axes provide insight into some of the flow control rules of the algorithm. The resulting skeletonization algorithm provides a discrete parametric representation of the axis of smooth simply connected shapes.

The next three sections address the three questions raised above. In Section 2 we address the problem of boundary reconstruction and show how we can use the new boundary representation to extract boundary features from the axis function. In Section 3 we present the local restrictions on the axis function. A theorem stating the main result of the section is cited, its proof appearing in the Appendix. In Section 4 we address the problem of axis generation and suggest a novel skeletonization approach. In Section 5 we present a highly accurate and quick skeletonization algorithm incorporating the suggested skeletonization approach. Skeletonization examples are presented. We conclude with a short summary in Section 6. The rest of the introduction is devoted to the notation and terminology that we use.

A medial axis of a simple planar shape is a collection of axis segments, each being a continuous three dimensional parametric function $\mathscr{M}(a) = (X(a), Y(a), R(a))^{\mathrm{T}}$. The first two coordinates of the medial axis function, $X(a)$ and $Y(a)$, are the parametric description of a planar curve, the third coordinate $R(a)$ being the radius or so-called ''quenching function.'' In the sequel we sometimes refer separately to the medial axis curve as $\mathscr{A}(a) = (X(a), Y(a))^{\mathrm{T}}$. The parameter a that we normally use is the standard arc-length parameter of the curve $\mathscr{A}$. If p is an arbitrary parameterization of $\mathscr{A}$, then

$$a(p) = \int_0^p \sqrt{X'^2(\tau) + Y'^2(\tau)}\, d\tau.$$

From now on we shall use subscripts to indicate derivatives; thus $R_a = \partial R/\partial a$ and $\mathscr{A}_a = \partial \mathscr{A}/\partial a$.

The trivial way to describe the shape S of a given axis function $\mathscr{M}$ is through the union of axis disks:

$$S = \bigcup_{a \in \mathrm{Domain}(\mathscr{M})} B_{\mathscr{M}}(a). \tag{1}$$

An axis disk $B_{\mathscr{M}}(a)$ is a disk of radius $R(a)$ centered on $(X(a), Y(a))^{\mathrm{T}}$. Of course, not every three dimensional parametric function is a legal axis function. In order for it to be one, it must be the axis of some shape. Since a union shape (1) is defined for every axis-like function, we may say that to be a legal axis function, an axis-like function must be the axis of its union shape, S.

2. RECONSTRUCTION

Suppose we have the medial axis of a certain shape and we want to reconstruct the shape. We can obtain the shape

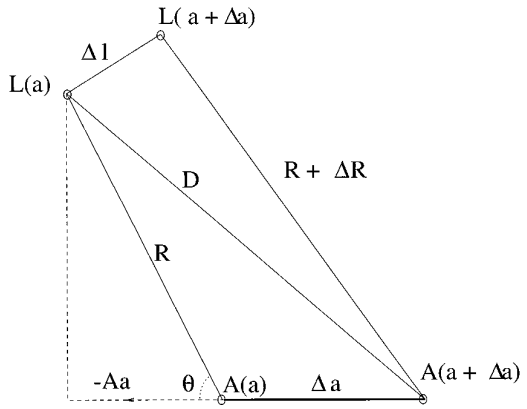

FIG. 1. The azimuth from the axis to the boundary.

using (1). This would give us an area description whose boundary we seek. We can, however, also reconstruct a boundary description of the shape directly from the axis description. This is made possible using a result by Blum.

In [2, 3], Blum asserted that each boundary point has at least one medial axis disk tangent to it, and that generically, each medial axis disk is tangent to the shape boundary at two points. Of the two points, one is located on the left of the medial axis and the other on its right. Blum also indicated that each of the two points is located at an angle $(180° - \theta)$ from the tangent to the axis so that

$$R_a(a) = \cos\theta. \tag{2}$$

Let us examine this statement in an intuitive way; an elegant argument based on differential geometry may also be found in [15]. Our proof of (2) appears in the appendix. Consider an infinitesimal axis segment as depicted in Fig. 1. The lower line segment in Fig. 1 is the infinitesimal axis segment, and the upper line segment is a corresponding segment of the boundary. The lines connecting the ends of the segments are the radii corresponding to the axis segments end points. Since the upper right triangle is nearly right angle, we can approximate

$$D^2 \approx \Delta l^2 + (R + \Delta R)^2.$$

The large lower triangle is right angle, hence also

$$D^2 = R^2 \sin^2\theta + (R\cos\theta + \Delta a)^2.$$

After second order infinitesimal terms are removed,

$$\Delta R = \Delta a \cos\theta,$$

which, in the limit, results in (2).

2.1. *Boundary from Medial Axis Description*

An axis point usually corresponds to two boundary points. Hence, an axis segment generically corresponds to two boundary segments, $\mathscr{L}(a)$ and $\mathscr{R}(a)$, located on the left side and on the right side of the medial axis respectively. A boundary point corresponding to the medial axis point with parameter a of the axis, is located at a distance $R(a)$ from the axis curve point $\mathscr{A}(a)$. The azimuth of the boundary point is θ degrees from the direction of the tangent $-\mathscr{A}_a(a)$ to the axis curve at a. Here θ is determined by (2). Hence, we have the following reconstruction formula

$$\begin{aligned}\mathscr{L} &= \mathscr{A} - R\begin{pmatrix} R_a & \sqrt{1-R_a^2} \\ -\sqrt{1-R_a^2} & R_a \end{pmatrix}\mathscr{A}_a \\ \mathscr{R} &= \mathscr{A} - R\begin{pmatrix} R_a & -\sqrt{1-R_a^2} \\ \sqrt{1-R_a^2} & R_a \end{pmatrix}\mathscr{A}_a.\end{aligned} \tag{3}$$

Note that $\mathscr{A}_a$ is a unit vector indicating a direction tangent to $\mathscr{A}$. The matrix multiplying it from the left is a unit size rotation matrix, rotating $\mathscr{A}_a$ by $\theta = \arccos R_a$ clockwise for $\mathscr{L}$ (or counterclockwise for $\mathscr{R}$). The directions obtained are the directions of $\mathscr{L}(a)$ and $\mathscr{R}(a)$ from the axis point $\mathscr{A}$. The distance to the boundary is the radius value $R(a)$.

The reconstruction formula (3) is formalized in the following lemma.

LEMMA 1. *If a segment of a* $\mathbf{C}^1$ *three dimensional parametric function is an axis segment, then the curves* $\mathscr{L}$ *and* $\mathscr{R}$ *of* (3) *are on the boundary of the shape the axis describes.*

The lemma is proven in the appendix. Relying on the above explanation of (3) the proof concentrates on proving (2).

The only exception to the above reconstruction rule is the case when either of the derivatives $R_a(a)$ or $\mathscr{A}_a(a)$ is not continuous. While the axis derivatives are not always continuous, the axis functions $R(a)$ and $\mathscr{A}(a)$ always are. Approaching a discontinuity at a_0 from one side of the axis, the boundary reaches a certain point in a direction corresponding to the limit value $(a \to a_0)$ of $R_a(a)$ and $\mathscr{A}_a(a)$ from that side. While approaching from the other side, the boundary similarly reaches a different point. Both points are, however, on the same circle of radius $R(a_0)$ centered on $\mathscr{A}(a_0)$. The gap between the two points is completed by a circular arc segment of this circle.

2.2. *Boundary Features from Medial Axis*

From the boundary description, boundary features are easily derived. The derivatives of (3) with respect to a are

$$\mathscr{L}_a = \left(\frac{1-R_a^2-RR_{aa}}{\sqrt{1-R_a^2}} + K_A R\right)\begin{pmatrix}\sqrt{1-R_a^2} & -R_a \\ R_a & \sqrt{1-R_a^2}\end{pmatrix}\mathscr{A}_a$$
$$\mathscr{R}_a = \left(\frac{1-R_a^2-RR_{aa}}{\sqrt{1-R_a^2}} - K_A R\right)\begin{pmatrix}\sqrt{1-R_a^2} & R_a \\ -R_a & \sqrt{1-R_a^2}\end{pmatrix}\mathscr{A}_a, \tag{4}$$

where K_A is the curvature of the axis curve $\mathscr{A}$. The unit tangent vectors to $\mathscr{L}$ and $\mathscr{R}$ are the derivatives of each curve segment with respect to its own arclength (l and r, respectively). From (4) it is easy to derive the left and right arclength information. Note that by the chain rule $\mathscr{L}_a = \mathscr{L}_l \cdot l_a$ and $\mathscr{R}_a = \mathscr{R}_r \cdot r_a$. $\mathscr{L}_l$ and $\mathscr{R}_r$ are both unit vectors, and l_a and r_a are the scalar length coefficients of $\mathscr{L}_a$ and $\mathscr{R}_a$, respectively. In (4), the vector part and the magnitude part are apparently easy to separate. Note that $\mathscr{A}_a$ multiplied by a rotation matrix is of unit length, and therefore

$$\mathscr{L}_l = \begin{pmatrix}\sqrt{1-R_a^2} & -R_a \\ R_a & \sqrt{1-R_a^2}\end{pmatrix}\mathscr{A}_a$$
$$\mathscr{R}_r = \begin{pmatrix}\sqrt{1-R_a^2} & R_a \\ -R_a & \sqrt{1-R_a^2}\end{pmatrix}\mathscr{A}_a. \tag{5}$$

The derivatives of the mappings of axis arclength into boundary arclengths are the scalar magnitude parts of (4),

$$l_a = \left(\frac{1-R_a^2-RR_{aa}}{\sqrt{1-R_a^2}} + K_A R\right)$$
$$r_a = \left(\frac{1-R_a^2-RR_{aa}}{\sqrt{1-R_a^2}} - K_A R\right). \tag{6}$$

If we differentiate (5) with respect to a, and divide the result by (6), we get the second derivatives of the boundary with respect to its arclength, the norm of which is the boundary curvature:

$$K_L = \frac{K_A\sqrt{1-R_a^2} - R_{aa}}{1-R_a^2-RR_{aa}+K_A R\sqrt{1-R_a^2}}$$
$$K_R = -\frac{K_A\sqrt{1-R_a^2} + R_{aa}}{1-R_a^2-RR_{aa}-K_A R\sqrt{1-R_a^2}}. \tag{7}$$

The radius of curvature of a boundary is the inverse of its curvature; hence

$$\rho_L = R + \frac{1-R_a^2}{K_A\sqrt{1-R_a^2} - R_{aa}}$$
$$\rho_R = R - \frac{1-R_a^2}{K_A\sqrt{1-R_a^2} + R_{aa}}. \tag{8}$$

The above results are not new. They correspond to results obtained by Blum and Nagel [3], who derived them geometrically. Nevertheless, the technique presented here makes possible the derivation of other (more complex) boundary features that do not have a simple geometric meaning, such as derivatives of the curvature or higher order derivatives of the boundary.

3. LOCAL RESTRICTIONS ON THE MEDIAL AXIS

As mentioned in the introduction, the way to verify that an axis-like function is indeed an axis of a shape is a global problem involving a reconstruction of the shape via either (1) or (3). The question raised in this section is to what extent local restrictions on the axis function can help us reject candidate axes. Two such local restrictions are intuitively apparent:

- The cosine in (2) is bounded to $[-1, 1]$. Hence the first restriction is

$$|R_a| \le 1. \tag{9}$$

- The arclength sign in (6) should always be positive (or more accurately, the tangent of the boundary cannot flip its direction), hence the second restriction:

$$1 - R_a^2 - RR_{aa} \ge |K_A| R\sqrt{1-R_a^2}. \tag{10}$$

Indeed the following lemmas are proven in the Appendix.

LEMMA 2. *If at a parameter value a_0 of an axis-like parametric function $|R_a| > 1$, then this function is not an axis function.*

LEMMA 3. *If at a parameter value a_0 of an axis-like parametric function $1 - R_a^2 - RR_{aa} < |K_A| R\sqrt{1-R_a^2}$, then this function is not an axis function.*

The next theorem formalizes the above two intuitive restrictions. The theorem is formally proven in the Appendix.

THEOREM. *Every medial axis obeys the above two restrictions* (9) *and* (10). *Consider an infinitesimally short 3D parametric* $\mathbf{C}^1$ *function* $(X(a), Y(a), R(a))$, *with a the*

arclength of $(X(a), Y(a))$. *If that segment obeys* (9) *and* (10) *with a strict inequality, it is a legal medial axis segment.*

The proof of the theorem is based on Lemmas 2, 3, and 4:

LEMMA 4. *If a parametric function obeys restrictions* (9) *and* (10) *with a strict inequality, then any axis disk is tangent to a boundary reconstruction as in* (3) *at two points. Also, the disk's curvature is larger then the reconstructed boundary's curvature at those points.*

4. AXIS REPRESENTATION

In this section we show that the axis function $\mathscr{M}$ of a shape is a solution of a system of ordinary differential equations. Note that the vector valued reconstruction formulae (3) constitute a system of four first order equations having the left and right boundary segment coordinates as inputs. This system should be enough to solve for the three unknown functions $X(a)$, $Y(a)$, and $R(a)$. In the following section we describe skeletonization as a solution of a system of differential equations.

We want to extract a description of the first order derivative of the axis function, $\mathscr{M}_a = (\mathscr{A}_a, R_a)$ from (3). Note that the vector $\mathscr{A}_a$ is unit length. We therefore only need to describe its direction.

The description of $\mathscr{M}_a$ will necessarily depend on the left and right boundaries $\mathscr{L}$ and $\mathscr{R}$. As in (3), the boundaries $\mathscr{L}$ and $\mathscr{R}$ in the description will be parameterized by the axis arclength parameter a. This causes a problem, since we assume that the boundaries $\mathscr{L}$ and $\mathscr{R}$ are given and represented in terms of their respective arclength parameters l and r. Every point on the boundaries corresponds to some point on the axis which is in turn parameterized by a. Therefore, we will have to describe l and r as functions $l(a)$ and $r(a)$ of a.

Taking the difference of the equations in (3) we have

$$\mathscr{L} - \mathscr{R} = 2R\sqrt{1 - R_a^2} \begin{pmatrix} 0 & -1 \\ 1 & 0 \end{pmatrix} \mathscr{A}_a.$$

Extracting the directional information of the above vector equation we get the equation describing the direction of $\mathscr{A}_a$,

$$\mathscr{A}_a \perp \mathscr{L} - \mathscr{R} \tag{11}$$

($\mathscr{A}_a$ is perpendicular to the segment connecting $\mathscr{L}$ and $\mathscr{R}$). We now sum $\mathscr{L}$ and $\mathscr{R}$ from (3) to get

$$\frac{2\mathscr{A} - (\mathscr{L} + \mathscr{R})}{2R} = R_a \mathscr{A}_a.$$

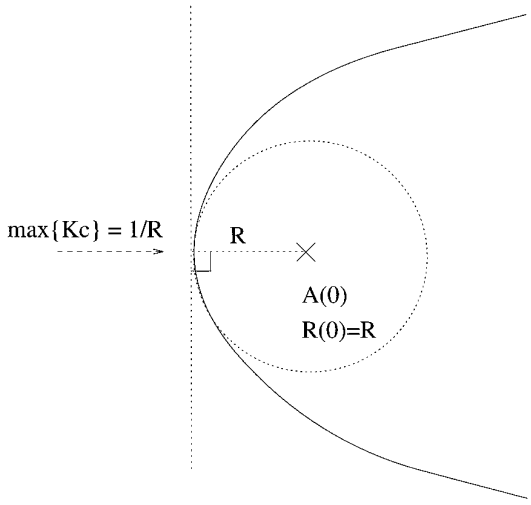

FIG. 2. The initial condition for the axis differential equation.

Considering the norm of the above vector equation we get

$$R_a = \frac{\|2\mathscr{A} - (\mathscr{L} + \mathscr{R})\|}{2R}. \tag{12}$$

Equations (11) and (12) describe the axis from corresponding boundary information $\mathscr{L}(l(a))$, $\mathscr{R}(r(a))$. To ensure that the correspondence between the boundary segments, and between them and the axis segment, is maintained, we need to simultaneously solve for $l(a)$ and $r(a)$. To do this we replace the axis terminology of (6) with boundary terminology, using (7), thereby obtaining

$$l_a = \sqrt{1 - R_a^2}\frac{1}{1 - K_L R} \quad r_a = \sqrt{1 - R_a^2}\frac{1}{1 - K_R R}. \tag{13}$$

The initial condition for the axis corresponds to Leyton's symmetry curvature duality [12]. The initial point is located normal to the boundary's curvature maximum, at a distance of $1/K_M$, where K_M is the maximal curvature; see Fig. 2. The initial condition for the radius parameter is the local radius of curvature $R(0) = 1/K_M$. The same point of maximal curvature on the boundary is the point where we "cut" the boundary, defining the two curves: $\mathscr{L}$ to the left of the axis and $\mathscr{R}$ to its right.

We have described the axis as the solution of a system of ordinary differential equations (11), (12), (13), and an initial condition. Starting at an initial condition we could, in theory, find the axis via a numerical solution of the system. Such a numerical solution would usually result in a series of densely spaced points on the axis (each complemented with the corresponding radius value). The implementation issues are discussed in the next section.

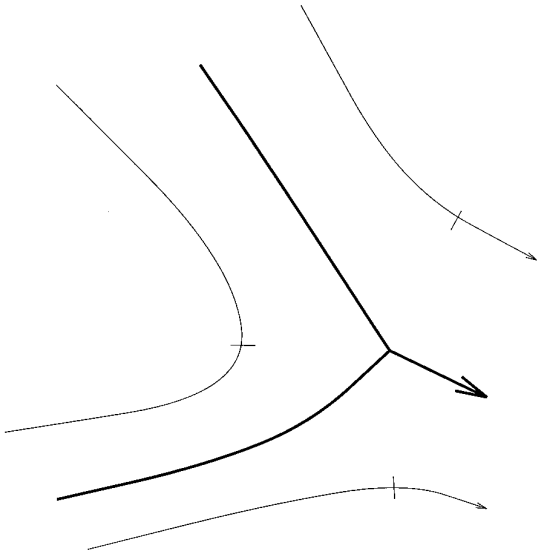

FIG. 3. Control of the axis generation at a junction.

5. THE SKELETONIZATION ALGORITHM

The application of the previously discussed results to a practical skeletonization algorithm faces two serious difficulties. The first problem is that the system of differential equations (11), (12), (13) is highly unstable. The second problem is that the above scheme refers to a single axis segment. To obtain the full axis of a shape some control process should be applied to the differential evolution of the axes in order to detect meeting axes segments, create a junction, and redirect the differential equation based axis generation process to derive the third branch of the junction; see Fig. 3. In this section we describe solutions to the two problems described above. The full details of the algorithm will not be described in this paper. Those may be found in a fully documented C program implementing the algorithm accessible by anonymous ftp from ftp.technion.ac.il in the directory/pub/supported/cs/misc/dorons.

The skeletonization algorithm is roughly divided into two processes: The generation process and the control process. The former solves the first problem via a stabilized implementation of the differential evolution equations for the axis. The latter solves the second problem of flow control.

The generation process is the "dumb" part of the algorithm. It is initiated with a valid pair of points on the boundary of the shape, i.e., two boundary points corresponding to an axis point. Once initiated it produces a series of equally spaced axis points along the axis segment. Calculating an axis point, the generation process is aware of no more then an infinitesimal region around the two corresponding boundary points.

The "smart" part of the algorithm is the control process. The control process considers global shape information. It first scans the boundary for positive local curvature maxima. Those curvature maxima are locations in which the control process initiates the generation process. The control process also keeps record of all the boundary segments scanned, and all the axis segments calculated so far by the generation process. The control process may interrupt the generation process, to either stop or redirect it.

5.1. *The Axis Generation Process*

Since Eqs. (11), (12), and (13) constitute a highly unstable differential equation system, it is impossible to implement the approach suggested in Section 4 directly. A stabilization process is necessary for implementation. Each step of the proposed skeletonization approach is therefore split into two phases: An estimation phase that relies on the differential equations, and a stabilizing phase that ensures that the axis location and the corresponding boundary parameters are accurate.

In the stabilizing phase we use a description of the symmetry set of planar shapes, proposed by Giblin and Brassett [8]. A symmetry set of a planar shape is a thin planar set that contains the medial axis. Like axis points, each point in the symmetry set corresponds to a pair of boundary points. Symmetry points that are also axis points correspond to the same pairs of boundary points the axis points correspond to. Giblin and Brassett [8] argued that the set of all valid pairs of boundary points corresponding to the symmetry set is the zero set of

$$\langle \mathscr{L}(l) - \mathscr{R}(r), \mathscr{L}_l(l) + \mathscr{R}_r(r) \rangle, \tag{14}$$

where $\langle \cdot, \cdot \rangle$ is the scalar product of vectors.

A valid pair of boundary points are boundary points whose distance from the intersection of their normals is equal. Given a valid pair of points on the boundary we estimate the next valid pair using (13). The parameters of the estimated valid pair initiate a simple search algorithm for the zeros of (14). Since the estimation phase is accurate enough, the zero search is very quick, and the accurate valid pair is close to the estimated pair. The location of the corresponding axis point is the intersection of normals to the boundaries $\mathscr{L}$ and $\mathscr{R}$ at the new valid pair. The radius function is the distance from the axis point to each of the boundary points.

It has to be noted that the estimation phase in the above scheme is important. Zero searching on (14) stabilizes the skeletonization only when the search is initiated close enough to the accurate value of the parameters. If for example, we replace the estimation via (13) with a simple incrementation of the parameters, we face serious convergence problems in the stabilization phase. The zero search

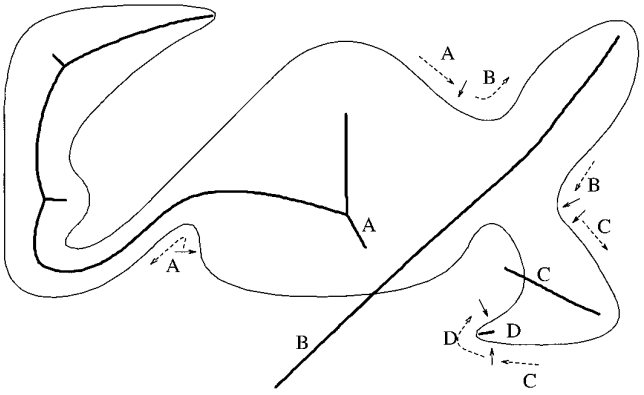

FIG. 4. Boundary and corresponding axis segments at an intermediate stage of the skeletonization algorithm.

always converges; however, it might take more iterations, and would sometimes converge to parameters corresponding to axis points that are far away from the previous axis point. Those convergence problems usually occur when the correct incrementation of the left side parameter is substantially different from the corresponding incrementation of the right side parameter. An additional consequence of the estimation via (13) is that the resulting axis points are generally equally spaced.

5.2. *The Control Process*

After scanning the boundary for local curvature maxima, the control process keeps a clockwise ordered list of pointers to boundary locations in which the generation process is to be initiated. From that point on, the control process "learns" the boundary curve only through the generation process. However, in contrast to the former, it keeps record of the information and does not "forget" it.

A generation process is sequentially started by the control at each positive curvature maximum. The generation process produces an axis segment and updates the control. The generation is stopped by the control if either of the stopping conditions described below is fulfilled. Once the axis generation is stopped, a new generation process is started at the next curvature maximum in the ordered list, unless the control decides the axis is complete.

The control process maintains a list of boundary segments scanned so far by the generation process. Every boundary segment corresponds to an axis segment or to a tree structure of axis segments, maintained separately by the control process; see Fig. 4. The axis corresponding to a scanned boundary segment is its axial description.

A new boundary segment is created whenever the generation process is initiated on a new curvature maximum. As the generation progresses, the boundary segment grows. When an active boundary segment meets an existing segment (e.g., the contact between boundary segments A and B or C and D in Fig. 4), the control interrupts the generation and declares a conflict situation. The conflict arises from the fact that a boundary point may correspond only to one axis segment. The conflict situation is resolved in three possible ways arbitrated by the relative size of the radius value at the two conflicting axis points:

• If the radius value of the active axis point is larger than the radius value of the older axis point, the generation process terminates. For example, Fig. 5a describes the intermediate stage when the active boundary segment B met an older segment A. The axis disks corresponding to the two segments touch the boundary at the end points of the segments. Since the boundary segments meet, the larger (new) axis disk contains the smaller (old) axis disk. Hence, it also contains a boundary point (the second end point of the old boundary segment). This implies that the larger

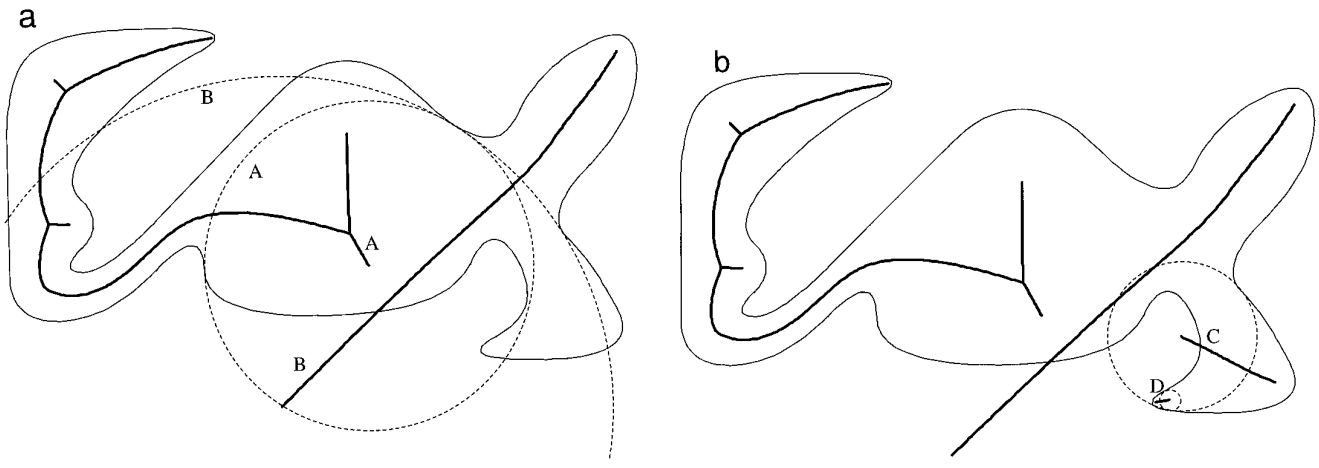

FIG. 5. Examples of conflicts where the radii are different.

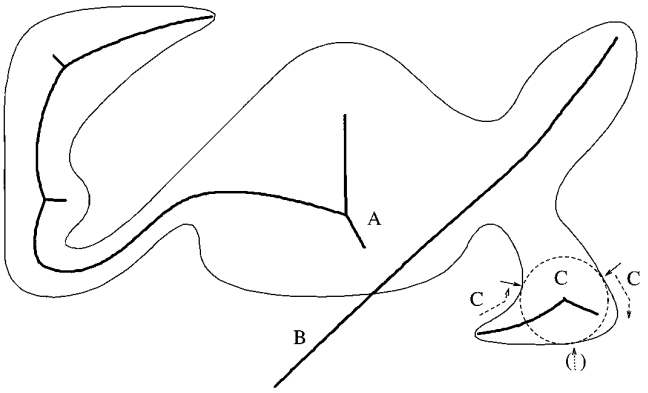

FIG. 6. Creation of a junction.

axis disk can not be a maximal disk in the shape. Hence, the new axis point is not recorded, and the generation process is terminated.

• If the radius value of the active axis point is smaller than the radius value of the older axis point, as in segments C and D of Fig. 5b, the older axis point is not part of the shape axis. Hence the axis point of the older axis segment is deleted. With its deletion, the corresponding boundary segment is shrunk.

• If both radius values are equal, the location of both axis points is the same. They are both located at the same distance in a direction normal to the common boundary segment. In this case the location is declared a junction, the two boundary segments are merged to one, and both axis segments are merged as branches of a tree structure whose root is a third axis segment that is initiated at the junction. The generation process is redirected to operate on a new valid pair of boundary points, the end points of the newly merged boundary segment, (see Fig. 6).

The control process stops the axis generation in three more cases:

• When the left and right boundary segments cannot support an axis segment any more. From the boundary's point of view, this situation may be detected when one of the boundary segments contains a twist that penetrates the previously calculated axis disk; see Fig. 7a. From the axis point of view this situation is indicated by an axis that does not obey restriction (10). Practically the situation is detected by the algorithm when the new parameters estimated to correspond to the next axis point via (13), retreat into the scanned boundary segment instead of advancing outward. Note that in Lemma 3 in the appendix we prove that if restriction (10) is not obeyed then necessarily either $l_a < 0$ or $r_a < 0$. This in turn implies that indeed one of the incrementations estimated by (13) will have the wrong sign.

• When the axis segment is obviously too long. A global control process can tell that an axis segment is obviously too long if it extends beyond the borders of the shape. To check whether a point is outside of a given shape is a difficult task. Therefore, we suggest to check only whether the axis is inside the frame of the shape. The frame of the shape is the box enclosing the maximal and minimal coordinate values of the boundary points. Clearly, the shape itself is inside its frame. In Fig. 7b axis segment B is stopped as it exceeds the frame of the shape. Note that in order to give the example of Fig. 5a (which is, by the way, quite rare), it was necessary to extend the frame of the shape.

• When the axis is complete. In this case the algorithm is stopped altogether. The axis is complete when the entire shape boundary has been scanned. Note that the end condition occurs before the list of curvature maxima is exhausted. This happens because the last axis segment is

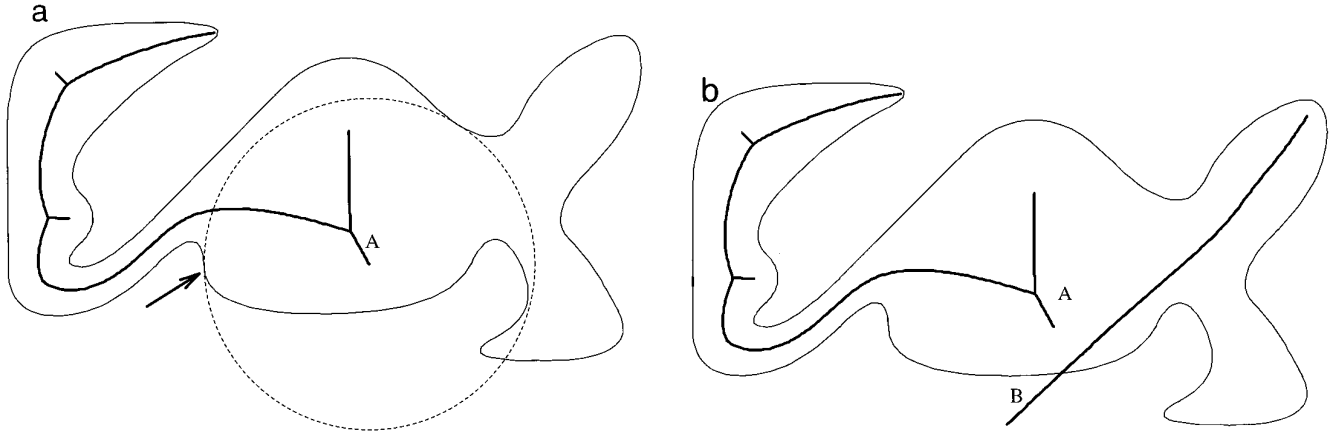

FIG. 7. Two situations in which the axis generation process is stopped.

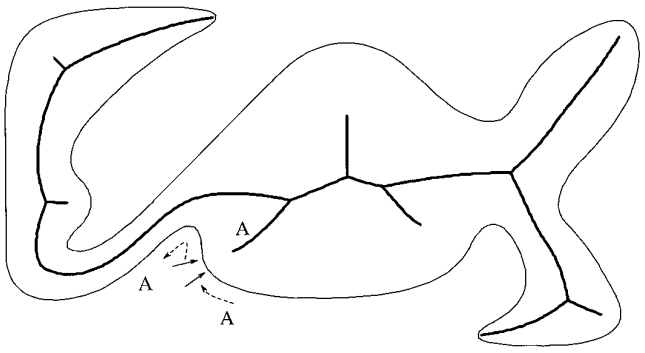

FIG. 8. End condition for the skeletonization algorithm.

developed from a junction towards a curvature maximum from which axis generation has not yet been initiated, as for example axis segment A in Fig. 8.

After stopping a generation process, the control process initiates a new generation process at the next curvature maximum. The fact that the curvature maxima which initiate the generation processes are ordered in a clockwise order is a key element in the control process. The results of the skeletonization algorithm are, however, invariant to the nature and location of the curvature maximum driving the first generation process. This includes curvature maxima that do not correspond to a free end of some axis in the final axis of the shape (a few such maxima appear in Fig. 9b). Note that in contrast to the medial axis, end points of the local symmetry axes described by Leyton [12] do reach *every* curvature extremum.

Figure 9 presents two examples of medial axes produced by the algorithm described above. The shapes in the figure are defined by spline boundaries.

6. SUMMARY

This paper is about a novel accurate skeletonization algorithm for shapes with smooth boundaries. Throughout this paper, we advocated a connection between the parametric descriptions of the boundary and the medial axis. This connection has been shown useful in calculating boundary features. It has also led to two necessary and locally sufficient restrictions on axis functions. We have proposed a new skeletonization approach determining the medial axis as a solution of a first order system of ordinary differential equation. Finally, we have applied parts of the proposed approach in a skeletonization algorithm for simply connected shapes whose boundaries are described via parametric curves.

As a final note we would like to stress again the importance of the smooth boundary input in the context of skeletonization. In the CAD community the need for accurate skeletonization techniques from smooth parametric boundary descriptors is quite clear because those are commonly used descriptors in CAD. The most common shape descriptor in computer vision is however the pixel. Indeed many skeletonization algorithms rely on pixel or polygonal inputs. Since the axis is a very unstable feature, especially when rough or edgy shapes are concerned, skeletonization algorithms produce unsatisfactory results especially when the input is pixel or polygonal data. Smoothing the data before skeletonization stabilizes the resulting axis considerably. The novelty in the skeletonization algorithm presented in this paper is in the smooth parametric boundary description it operates on.

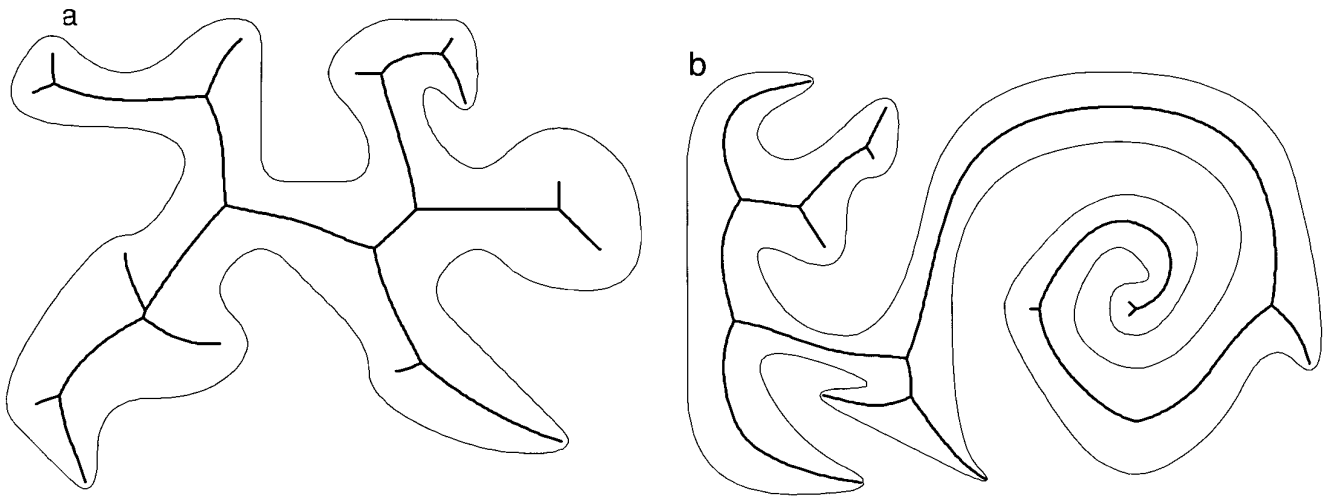

FIG. 9. Results of the skeletonization algorithm.

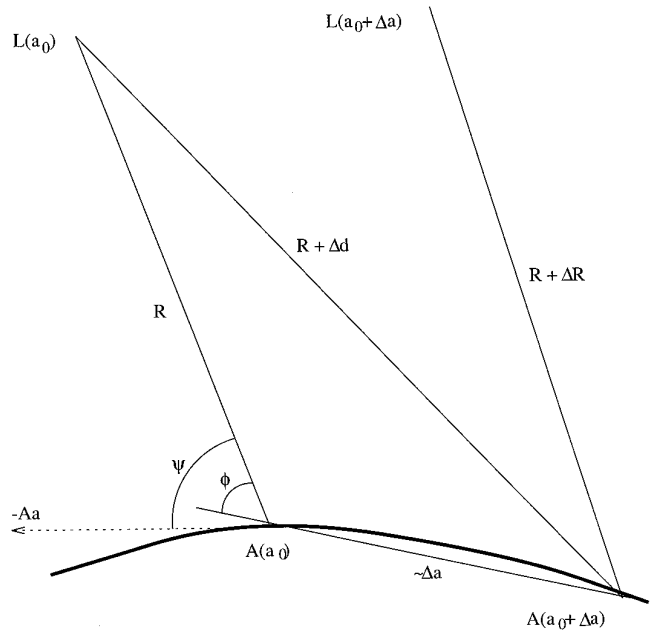

FIG. 10. The azimuth of the boundary from the axis point corresponding to it.

APPENDIX

LEMMA 1. *If a segment of a* $\mathbf{C}^1$ *three dimensional parametric function is an axis segment, then the curves* $\mathscr{L}$ *and* $\mathscr{R}$ *of* (3) *are on the boundary of the shape that the axis describes.*

Remark. An elegant argument based on differential geometry may be found in [15].

Proof. Every axis disk touches the boundary of the shape at two points. Those points are $R(a)$ distant from the axis point $\mathscr{A}(a)$. The only exceptions to the two point correspondence may be found at the axis end point. (Explanations about boundary axis point correspondences, may be found in [2], and more formally in [8] and [9]). What we shall show is that the azimuth of the boundary points on the disk, is the angle θ on both sides of the tangent $\mathscr{A}_a$ to the axis curve, with θ as in (2).

Let us assume the contrary, and suppose that the azimuth of a boundary point is at angle ψ from $\mathscr{A}_a$, such that $\psi > \theta$ with $\cos\theta = R_a$. Since the tangent $\mathscr{A}_a$ to the axis is continuous, for a sufficiently small Δa also the angle ϕ of the azimuth from the infinitesimal line segment connecting axis points a and $a + \Delta a$ will be, such that $\phi > \theta$. See Fig. 10.

We have $\cos\phi < \cos\theta = R_a$. Since R_a is also continuous, we can find a sufficiently small Δa so that

$$\frac{\Delta R}{\Delta a} > \cos\phi, \tag{15}$$

where $\Delta R = R(a + \Delta a) - R(a)$.

Let us examine the distance $R + \Delta d$ from $\mathscr{A}(a + \Delta a)$ to $\mathscr{L}(a)$. By the cosine law,

$$(R + \Delta d)^2 = R^2 + \Delta a^2 - 2R\Delta a \cos(180° - \phi).$$

Removing second order infinitesimal terms, we get

$$\frac{\Delta d}{\Delta a} = \cos\phi. \tag{16}$$

From (15) and (16),

$$\Delta d < \Delta R$$

Therefore, points lying on the azimuth $\psi > \theta$ from $\mathscr{A}_a$, are inside the axis disk of a neighboring points, contradicting the assumption that it is a boundary point of the shape.

A similar argument is valid for the assumption of an azimuth $\psi < \theta$. ■

LEMMA 5. *Let* $\overline{AB}$ *and* $\overline{CD}$ *be two segments in the plane, intersecting at a point E. Then either* $B \in C_C^D$ *or* $D \in C_A^B$, *where* C_A^B *denotes the circle centered at A and passing through B, and* C_C^D *denotes the circle centered at C and passing through D.*

Proof. We have to show (see Fig. 11), that either $BC \leq CD$ or $DA \leq AB$. Suppose the contrary is true, i.e. $BC > CD$ and $DA > AB$. adding the two inequalities we get $BC + DA > CD + AB = CE + ED + AE + EB =$

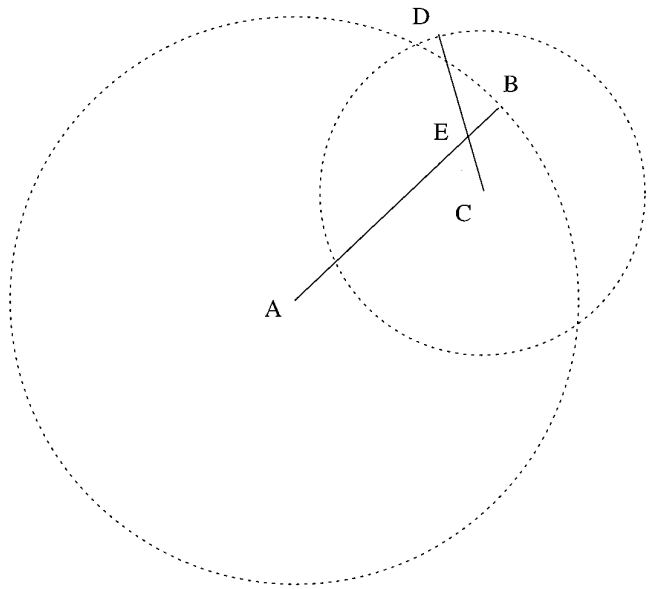

FIG. 11. If the radii intersect, at least one of their end points is inside the other circle.

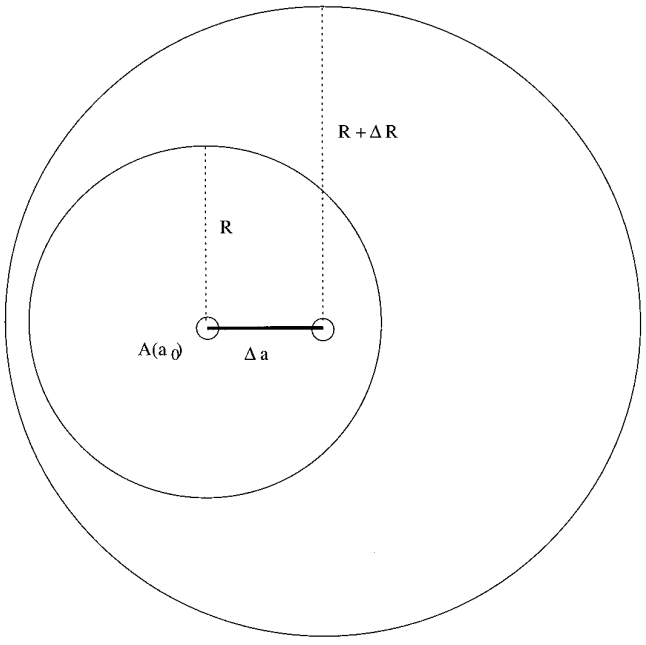

FIG. 12. If the radius function changes too quickly, the proposed function can not be an axis function.

(CE + EB) + (DE + EA) in contradiction to the triangle inequality BC ≤ CE + EB and DA ≤ DE + EA. ■

THEOREM. *Every medial axis obeys* (9) *and* (10). *Consider an infinitesimally short* 3*D parametric* $\mathbf{C}^1$ *function* $(X(a), Y(a), R(a))$, *with a the arclength of* $(X(a), Y(a))$. *If that segment obeys* (9) *and* (10) *with a strict inequality*, *it is a legal medial axis segment*.

We separate the theorem into a few lemmas.

LEMMA 2. *If at a parameter value* a_0 *of an axis-like parametric function* $|R_a| > 1$, *then this function is not an axis function*.

Proof. Suppose $R_a(a_0) > 1$; then for a sufficiently small Δa, we have $\Delta R/\Delta a > 1$, with $\Delta R = R(a_0 + \Delta a) - R(a_0)$. Since $\Delta R > \Delta a$, the axis disk of parameter a_0, is totally contained in the axis disk of parameter $a_0 + \Delta a$. See Fig. 12.

A similar argument can be made for the assumption $R_a < -1$. ■

LEMMA 3. *If at a parameter value* a_0 *of an axis-like parametric function*, $1 - R_a^2 - RR_{aa} < |K_A|R\sqrt{1 - R_a^2}$, *then this function is not an axis function*.

Proof. Suppose the contrary is correct, and the function is an axis function. By Lemma 1 the curves $\mathscr{L}$ and $\mathscr{R}$ in (3) are on the boundaries of the shape corresponding to the axis function. Consider the line segment connecting the axis point $\mathscr{A}(a_0)$ to $\mathscr{L}(a_0)$, the left boundary point corresponding to it according to (3). Now extend the line segment to a line (the dotted line in Fig. 13), obtaining two half planes. By (5), the tangent $\mathscr{L}_l$ to the $\mathscr{L}$ at a_0, is pointing toward the same half plane as $\mathscr{A}_a$ (the tangent to $\mathscr{A}$). However, the derivative $\mathscr{L}_a$ in (4) is pointing to the same side only if l_a in (6) is positive.

Suppose, however, that $l_a < 0$. Then, for a sufficiently small Δa, the radius connecting the axis point at parameter $a_0 + \Delta a$ on one side of the line to the boundary point $\mathscr{L}(a_0 + \Delta a)$ on the other side of the line intersects it; see Fig. 13. According to Lemma 5 this means that either $\mathscr{L}(a_0)$ is in the axis disk of parameter $a_0 + \Delta a$ or $\mathscr{L}(a_0 + \Delta a)$ is in the axis disk of parameter a_0. Hence, either $\mathscr{L}(a_0)$ or $\mathscr{L}(a_0 + \Delta a)$ is not a boundary point, contradicting the assumption that the function is an axis function.

A similar argument can be made for $r_a < 0$. Note that if $1 - R_a^2 - RR_{aa} < |K_A|R\sqrt{1 - R_a^2}$, as in the hypothesis of the lemma, then by (6) either $l_a < 0$ or $r_a < 0$. ■

LEMMA 4. *If a parametric function obeys restrictions* (9) *and* (10) *with a strict inequality*, *then any axis disk is tangent to a boundary reconstruction as in* (3) *on two points*. *The disk's curvature in this case is larger than the reconstructed boundary's curvature at those points*.

Proof. First note that a boundary reconstruction is possible only for parametric functions obeying (9); otherwise the expressions in (3) do not exist.

From the reconstruction equations it is evident that every axis disk touches the reconstructed boundary at two points. The disk centered at $\mathscr{A}(a)$ touches the left and

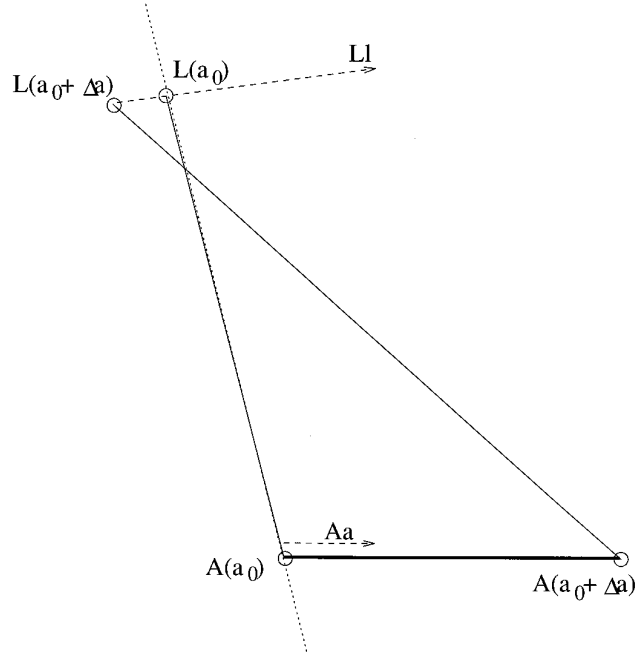

FIG. 13. Boundary parameter is monotone in axis parameterization.

right boundary segments at $\mathscr{L}(a)$ and $\mathscr{R}(a)$ respectively. The tangent vectors to the boundary segments in (5) are perpendicular to the directions of their respective axis disk radii. Those are given by substituting (3) into $(1/R)$ $(\mathscr{L} - \mathscr{A})$ and $(1/R)$ $(\mathscr{R} - \mathscr{A})$. Hence every axis ball is tangent to the boundary at two points. (The points are different or else $R_a = 1$.)

To prove the second part of the lemma we have to show that the axis disk curvature $(1/R)$ is larger then both boundary curvatures K_L and K_R in (7). If either of the boundary curvatures is negative, then the respective problem is solved. Therefore, we show that if $K_L > 0$ then $\rho_L > R$ and if $K_R > 0$ then $\rho_R > R$.

If

$$K_L = \frac{K_A\sqrt{1 - R_a^2} - R_{aa}}{1 - R_a^2 - RR_{aa} + K_A R\sqrt{1 - R_a^2}} > 0$$

then from restriction (10) the denominator is positive, and

$$K_A\sqrt{1 - R_a^2} - R_{aa} > 0. \tag{17}$$

We have to show that in this case $\rho_L > R$ or, by substitution from (8),

$$\frac{1 - R_a^2}{K_A\sqrt{1 - R_a^2} - R_{aa}} > 0.$$

But this is a direct conclusion from (17) and the restriction (9).

A similar argument asserts that if $K_R > 0$ then $\rho_R > R$. ■

Proof of the Theorem. The first part of the theorem is: All axis functions obey (9) and (10). This part is directly derived from Lemmas 2 and 3.

The second part is: An infinitesimal axis like function $\mathscr{M}$ obeying (9) and (10) with a strict inequality is a legal axis function. In order to show this, we have to show that $\mathscr{M}$ is the axis of its union shape (1).

Let us first describe a shape by its boundary. The boundary is composed of the two boundary segments $\mathscr{L}$ and $\mathscr{R}$ defined by the reconstruction equations (3), and of two arc segments connecting them at both ends (the arc segments of the disks at the ends of the proposed infinitesimal axis). Next we show that the boundary described above is the boundary of the union shape. The boundary is closed. Furthermore, since each boundary point is on the boundary of at least one axis disk, none of the points of the boundary described above is outside the union shape. What remains to be shown is that non of the boundary points is inside the union shape, or equivalently, non of the points is inside any of the axis disks.

From Lemma 4, all proposed axis disks are tangent to the boundary, and the radius of curvature at every boundary point is larger then the radius of the axis disk touching it. Therefore, the constructed boundary points are outside the axis disks corresponding to neighboring boundary points. Since the axis segment is infinitesimal, we conclude that every point of the boundary is outside all other axis disks of the axis segment. Hence, the boundary constructed above is the boundary of the union shape.

Since all the disks of the proposed axis touch the boundary at two different points, they are all maximal disks in the union shape. The proposed axis function describes therefore a collection of centers of maximal disks. All that is left to be shown is that the collection is complete, and that there exists no other maximal disk in the union shape.

Assume the contrary is correct, and there is another maximal disk in the union shape. Being a maximal disk it has to either touch the boundary at two different points, or at one point in which case, its radius has to be equal to the radius of curvature at that point. In any case, the maximal disk has to be tangent to the boundary at the touching points.

If an internal disk touches a point of the two arc segments connecting $\mathscr{L}$ with $\mathscr{R}$, its radius is bound to be less than or equal to the radius of the axis disk at the corresponding end of the axis segment. Hence, such a disk may not be a maximal disk. If an internal disk touches a point of either $\mathscr{L}$ or $\mathscr{R}$, it has to be tangent to the boundary at the point. Also, the axis disk corresponding to the same point is tangent to the boundary. Hence, either the new maximal disk contains the axis disk or vice versa. In both cases we get a contradiction to the assumptions.

The only alternative allowing the two disks to be simultaneously maximal in the union shape is a negative discontinuity of the tangent at the relevant boundary point. In this case both disks may be "tangent" to the boundary but not to each other; see Fig. 14. The boundary point is then a

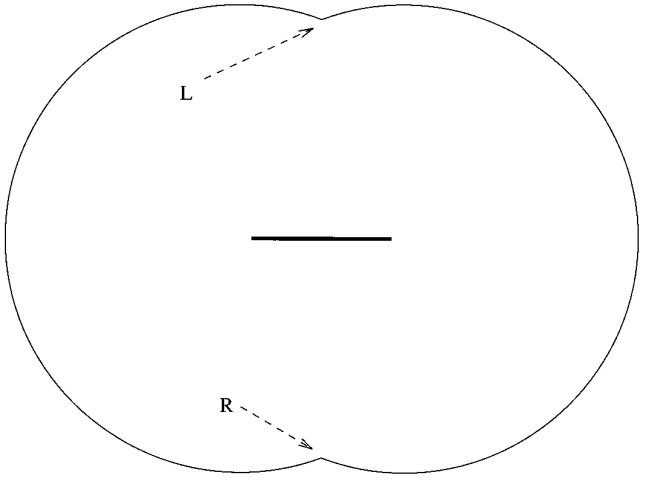

FIG. 14. An example of a union shape with a concave "corner."

concave ''corner.'' The situation described above is, however, not possible under the assumptions, since a concave corner in the boundary corresponds to an axis of nontrivial length. (The end points of the axis segment corresponding to a concave corner are located in a direction perpendicular to the boundary's tangents from both sides). In such cases, we therefore have $l_a = r_a = 0$. From (6) it is evident that this implies that (10) is true with equality, in contradiction to the assumptions. ■

REFERENCES

1. C. Arcelli, Pattern thinning by contour tracing, *Comput. Graphics Image Process.* **17,** 1981, 130–144.
2. H. Blum, Biological shape and visual science, I, *J. Theor. Biol.* **38,** 1973, 205–287.
3. H. Blum and R. N. Nagel, Shape description using weighted symmetric axis features, *Pattern Recognition* **10,** 1978, 167–180.
4. F. L. Bookstein, The line skeleton, *Comput. Graphics Image Process.* **11,** 1979, 123–137.
5. J. W. Brandt and V. R. Algazi, Continuous skeleton computation by Voronoi diagram, *CVGIP Image Understanding* **55,** 1992, 329–338.
6. J. W. Bruce and P. J. Giblin, Growth, motion and 1-parameter families of symmetry sets, *Proc. R. Soc. Edinburgh Sect. A* **104,** 1986, 179–204.
7. A. R. Dill, M. D. Levine, and P. B. Noble, Multiple resolution skeletons, *IEEE Trans. Pattern Anal. Mach. Intell.* **9,** 1987, 495–504.
8. P. J. Giblin and S. A. Brassett, Local symmetry of plane curves, *Am. Math. Monthly* **92,** 1985, 689–707.
9. P. J. Giblin and D. B. O'Shea, The bitangent sphere problem. *Am. Math. Monthly* **97,** 1990, 5–23.
10. R. Kimmel, D. Shaked, N. Kiryati, and A. M. Bruckstein, Skeletonization via Distance Maps and Level Sets, *Comput. Vision Image Understanding* **62,** 1995, 382–391.
11. D. T. Lee, Medial axis transformation of a planar shape, *IEEE Trans. Pattern Anal. Mach. Intell.* **4,** 1982, 363–369.
12. M. Leyton, *Symmetry Causality Mind,* MIT Press, Cambridge, MA, 1992.
13. U. Montanari, Continuous skeletons from digitized images, *J. Assoc. Comput. Mach.* **16,** 1969, 534–549.
14. H. Persson, NC machining of arbitrarily shaped objects, *Comput. Aided-Design* **10,** 1978, 169–174.
15. J. Ponce, On characterizing ribbons and finding skewed symmetries, *Comput. Vision Graphics Image Process.* **52,** 1990, 328–340.
16. A. Rosenfeld, Axial representations of shape, *Comput. Vision Graphics Image Process.* **33,** 1986, 156–173.
17. C. K. Yap and H. Alt, Motion planning in the CL-environment, in *Lecture Notes in Computer Vision,* vol. 382 (F. Dehne, J. R. Sack, and N. Santoro, Eds.), pp. 373–380, Springer-Verlag, Berlin/New York, 1989.